University of Wollongong

Research Online

Faculty of Science, Medicine and Health - Papers: part A

Faculty of Science, Medicine and Health

2012

Electrodeposition of pyrrole and 3-(4-tert-butylphenyl)thiophene copolymer for supercapacitor applications

Binbin Yue
University of Wollongong

Caiyun Wang
University of Wollongong, caiyun@uow.edu.au

Pawel Wagner
University of Wollongong, pawel@uow.edu.au

Yang Yang
University of Wollongong, yy922@uowmail.edu.au

Xin Ding
Donghua University

See next page for additional authors

Follow this and additional works at: https://ro.uow.edu.au/smhpapers

Part of the Medicine and Health Sciences Commons, and the Social and Behavioral Sciences Commons

Recommended Citation

Electrodeposition of pyrrole and 3-(4-tert-butylphenyl)thiophene copolymer for supercapacitor applications

Abstract

The electropolymerization of pyrrole (Py), 3-(4-tert-butylphenyl)thiophene (TPT) monomer or the mixed Py and TPT monomers on stainless steel mesh substrate were performed in 1 M LiClO4/acetonitrile solution. A much lower potential of 0.75 V was required for the co-electropolymerization of Py and TPT, in sharp contrast to that of 1.20 V for poly(3-(4-tert-butylphenyl)thiophene) (PTPT) formation. The resultant homopolymers and copolymer were characterized with FESEM and FTIR, and assembled into supercapacitors to investigate their electrochemical performances. The copolymer electrode delivered the highest specific capacitance of 291 F g−1 at a scan rate of 5 mV s−1, in comparison with that of 216 and 26 F g−1 for PPy and PTPT, respectively. This copolymer also exhibited a greatly improved cycling stability − only 9% of capacitance decrease was observed after 1000 charging−discharging cycles at a current density of 5 A g−1, while the capacitance losses for PPy and PTPT were 16% and 60%, respectively.

Keywords

tert, butylphenyl, thiophene, electrodeposition, applications, supercapacitor, pyrrole, 3, 4, copolymer

Disciplines

Medicine and Health Sciences | Social and Behavioral Sciences

Publication Details

Authors

Binbin Yue, Caiyun Wang, Pawel Wagner, Yang Yang, Xin Ding, David L. Officer, and Gordon G. Wallace

Electrodeposition of pyrrole and 3-(4-*tert*butylphenyl)thiophene copolymer for supercapacitor applications

Binbin Yue, [1, 2] Caiyun Wang,[2] Pawel Wagner,[2] Yang Yang,[2] Xin Ding[1], David L. Officer[2] and Gordon G. Wallace[2,*]

[1] Key Laboratory of Textile Science & Technology,

Ministry of Education of China,

Donghua University, Shanghai 201620, China.

[2] ARC Centre of Excellence for Electromaterials Science,

Intelligent Polymer Research Institute,

AIIM Facility, Innovation Campus,

University of Wollongong, NSW 2522, Australia.

*Prof. G. G. Wallace, corresponding author.

Tel.: +61 2 4221 3127; fax: +61 2 4221 3114.

E-mail address: gwallace@uow.edu.au(G.G. Wallace).

1

ABSTRACT

The electropolymerization of pyrrole (Py), 3-(4-*tert*butylphenyl)thiophene (TPT) monomer or the mixed Py and TPT monomers on stainless steel mesh substrate were performed in 1 M LiClO$_4$/acetonitrile solution. A much lower potential of 0.75 V was required for the co-electropolymerization of Py and TPT, in sharp contrast to that of 1.20 V for poly(3-(4-*tert*butylphenyl)thiophene) (PTPT) formation. The resultant homopolymers and copolymer were characterized with FESEM and FTIR, and assembled into supercapacitors to investigate their electrochemical performances. The copolymer electrode delivered the highest specific capacitance of 291 F g^{-1} at a scan rate of 5 mV s^{-1}, in comparison with that of 216 and 26 F g^{-1} for PPy and PTPT, respectively. This copolymer also exhibited a greatly improved cycling stability- only 9% of capacitance decrease was observed after 1000 charging-discharging cycles at a current density of 5 A g^{-1}, while the capacitance losses for PPy and PTPT were 16% and 60%, respectively.

KEYWORDS: Pyrrole, 3-Arylthiophene, Copolymerization, Electrode materials, Supercapacitors.

1.   Introduction

There is currently a great demand for the development of inexpensive, flexible or bendable, light-weight and environmentally friendly energy storage devices for portable equipment [1]. Being an important power source, supercapacitors possess the advantages of high power densities and excellent cycling stability. They are gaining increasing interest in the application of light weight, ultrathin energy management devices for wearable electronics [2].

Inherently conducting polymers (ICPs) are interesting candidates for flexible energy storage devices due to their relatively high theoretical capacities and the fact that they are light weight and flexible [1, 3-6]. However, as an electrode material for supercapacitor application, ICPs still have several limitations including poor cycling stability and high self-discharge due to the low doping degrees attainable [1, 6, 7]. There are two main strategies applied to overcome these drawbacks. One is the formation of composites with other substances such as metal oxides or carbon based materials [8-10]. Another promising method is the copolymerization of different types of monomers, which results in copolymers with better and controlled properties overcoming the limitations usually associated with homopolymers [11-14].

Copolymers of thiophene (Th) with 3,4-ethylenedioxythiophene (EDOT) [15] have been prepared by direct electrochemical oxidation of mixtures of the corresponding monomers and studied as electrodes in lithium cells. The corresponding copolymers showed better charge capacity, stability and response rate than pure PTh. Almost 100% capacity recovery was observed for poly(Th–EDOT) (1/1) copolymer after 25 cycles of CV scans at a scan rate of 50 mV s^{-1}, compared with that of ~40% and ~10% loss for PTh and PEDOT, respectively. Poly(pyrrole-co-aniline) exhibited much higher specific capacitance (489 F g^{-1}) than polypyrrole (163

F g^{-1}) and polyaniline (246 F g^{-1}) in 1 M Na$_2$SO$_4$ at a current density of 10 mA cm^{-2} in a three-electrode cell with a platinum counter electrode and a standard calomel reference electrode [16]. It is believed that the best practice test methods accurately predicting a material's supercapacitor performance is from a two electrode system [17]. To this end, we report the electrochemical copolymerization of pyrrole (Py) with 3-(4-*tert*butylphenyl)thiophene (TPT). In this work, a two electrode cell configuration was applied to obtain a more accurate determination of its supercapacitor performance.

Homopolymers or copolymers can be prepared via a chemical or electrochemical route. Compared with the chemical process, electrochemical polymerization can provide better control of film thickness and morphology; also, the material may be deposited *in situ* onto conductive substrates directly [18-20]. In this work, the homopolymers and copolymer were prepared by using a galvanostatic current method. The resulting copolymer demonstrated superior electrochemical properties to either PPy or PTPT, including higher specific capacitance and better cycling stability. A copolymer electrode delivered the highest specific capacitance of 291 F g^{-1} at a scan rate of 5 mV s^{-1}, in comparison with that of 216 and 26 F g^{-1} for PPy and PTPT, respectively. The copolymer electrode also displayed a smaller capacitance loss of 9% after 1000 charging-discharging cycles at a current density of 5 A g^{-1}, while the capacitance loss for PPy and PTPT was 16% and 60%, respectively.

2.   Experimental

2.1 Synthesis of the monomer 3-(4-*tert*butylphenyl)thiophene

Pyrrole was freshly distilled and stored in a freezer (-18 °C) before use, while all other chemicals were used as supplied.

3-(4-*Tert*butylphenyl)thiophene (TPT) has been synthesized by Suzuki coupling of 3-bromotiophene and 4-*tert*butylphenylboronic acid in dimethoxyethane. Potassium carbonate was used as a base and palladium tetrakis(triphenylphosphine) as a catalyst [21]. Our approach differs from previously reported where 3-thiopheneboronic acid and 4-bromo-*tert*butylbenzene were used as starting materials instead [22]. The analytical data of the compound was in agreement with that previous report [22]. The schematic structure of 3-(4-*tert*butylphenyl) thiophene (TPT) is shown in Scheme 1.
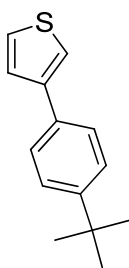
Scheme 1. Schematic structure of 3-(4-*tert*butylphenyl)thiophene (TPT)

2.2 Copolymerization

The monomers were galvanostatically electropolymerized to form the resultant homopolymers and copolymers. The working and counter electrodes were stainless steel mesh (Hongye Stainless Steel Wire Cloth Co. Ltd.), while the reference electrode was 0.01 M Ag/Ag$^+$ in 0.1 M TBAP in acetonitrile (ACN). The galvanostatic polymerizations were carried out with an applied current of 0.5 mA cm^{-2} for 600 s in a de-oxygenated acetonitrile solution containing 0.02 M monomers and 0.1 M LiClO$_4$. The molar ratio of monomers was 1:1 to form the copolymer. After polymerization, the polymer coated stainless steel sheets were washed thoroughly with acetonitrile to remove any residue. A free-standing film was used for FT-IR test, and it was prepared by being electrodeposited onto ITO glass for 1 h followed by

peeling off the substrate.

2.3 Physical characterization

The surface morphologies of the resultant copolymer and homopolymers were investigated by means of a cold-gun field emission scanning electron microscope (FESEM, JEOL JSM7500FA). FT-IR spectra were recorded on a FT-IR spectrometer (IRpretige-21, SHIMADZU) over the range from 750 cm^{-1} to 2000 cm^{-1}. Elemental analysis (%): C 38.62, N 11.05, S 0.30 and Cl 13.40.

2.4 Electrochemical characteristics

PPy, PTPT and the copolymer films were dried in a vacuum oven at 60ºC overnight, and the electrodes were assembled into LR 2032 type coin cells in a glove box. The electrolyte and separator were provided by CAP-XX (Australia). The electrolyte was 1 M tetraethylammonium tetrafluoroborate (TEATFB) in acetonitrile. Cyclic voltammetry was performed using a Solartron SI 1287 and scanned between 0 V and 1.5 V. Electrochemical impedance spectra were measured potentiostatically using a PCI4/750 Potentiostat/Galvanostat/ZRA (Gamry Instruments, Inc. USA). The frequency range was from 100 kHz to 0.01 Hz with an AC perturbation of 10 mV at the open circuit potential. Galvanostatic charge/discharge cycling tests for the cells were performed between 0 V and 1.5 V using a battery-testing device (Neware Electronic Co., China).

3.   Results and discussions

3.1 Electropolymerization of polymers

The chronopotentiogram (Fig. 1) exhibited an initial spike due to charging of the double layer and oxidation of monomer, followed by a slowly decreasing potential

as polymer growth proceeded. The decreasing potential was indicative of conducting polymer deposition on the electrode [23]. It is noted that the Py was oxidized and rapidly reached a steady potential at 0.628 V (Fig. 1iii), revealing that the polymer monolayer and nucleation sites were formed rapidly, and the growth stage was reached immediately [24]. For TPT monomer (Fig. 1i), initial fluctuation could be noticed prior to approaching the steady potential of 1.225 V, revealing that these two polymers were probably formed via different electropolymerization mechanisms. The chronopotentiogram of the co-monomers was similar to that of Py monomer (Fig. 1ii), the potential decreased sharply to 0.733 V, much lower than that of 1.225 V for PTPT polymerization but slightly higher than that for PPy (0.628 V).

3.2 Surface morphology of polymers

Fig. 2 shows the surface morphology of PPy, copolymer and PTPT coated stainless steel mesh. PPy shows a cauliflower-like nodule structure composed of microspherical grains as reported previously [24] (Fig. 2a and d). In contrast, PTPT shows a more even surface but with deep troughs under low magnification (Fig. 2c). This polymer appeared to have a flocculent structure under high magnification (Fig. 2f), which might be due to the different polymer growth mechanism for PTPT and PPy as revealed by the chronopotentiograms. Such flocculent structure of PTPT can result in a high surface area. The surface of the copolymer displayed a similar structure as PPy but with more evenly distributed microsperical grains (Fig. 2b, 2e). This resulted in higher surface area being available.

3.3 Infrared spectroscopy of polymers

FT-IR spectra of PTPT, PPy and copolymer are shown in Fig. 3. According to the spectrum of PTPT (Fig. 3i), the bands at 1477 and 1373 cm^{-1} are contributed to the C–C and C=C stretching of the thiophene ring, respectively [13].The band at 817

cm^{-1} may be assigned to C–S stretching vibration [25]. The bands at 1508 cm^{-1} and 1427 cm^{-1}in the spectrum of PPy (Fig. 3iii) are related to the C–C and C–N stretching vibrations in the pyrrole ring, respectively. The broad band from 1400 to 1250 cm^{-1} was attributed to C-H or C-N in-plane deformation modes and had a maximum at around 1265 cm^{-1}. In the region from 1250 to 1100 cm^{-1}, corresponding to the breathing vibration of the pyrrole ring, the peak was situated at around 1123 cm^{-1}. The band of C-H and N-H in plane ring deformation vibration was situated at 995 cm^{-1}. The peaks at 957 cm^{-1} could be attributed to C-C out of plane ring deformation vibration [26]. Copolymer exhibits bands at 1508, 1276 and 1130 cm^{-1} (Fig. 3ii) are characteristic bands from pyrrole units. The bands at 1346 and 810 cm^{-1}, originating from thiophene rings, can also be found. This is a clear evidence of the co-existence of Py units and TPT units in the copolymer.

3.4 Supercapacitor performance of polymer electrodes

The performance of supercapacitor cells composed of PTPT, PPy and copolymer electrodes were evaluated by cyclic voltammetry (CV) over the potential range of 0-1.5 V. The corresponding CV curves at different scan rates from 5 to 500 mV s^{-1} are shown as Fig. 4a, b and c, respectively. All the CVs of these three types of polymer supercapacitors displayed rectangular areas, indicative of good double-layer capacitive behaviour [27]. The copolymer and PPy electrode both displayed a decreased current at high voltage, which might be explained by a redox process taking place at the limits and beyond a given potential range which could lead to the formation of passive layers of poor conductivity [28]. No such phenomenon was observed for PTPT, which still kept its rectangular shape even at 500 mV s^{-1}. This might be derived either from purely double-layer capacitive behaviour or rapid Faradaic reaction. It is noticed that the current generated at the high voltage from

PTPT at a scan rate of 100 mV s^{-1} was much lower than copolymer and PPy (Fig. 4d), indicative of the limited Faradaic contribution over the whole scan range. The largest integrated area under the respective voltammetric waves for copolymer is an indication of the highest available charge/discharge capacitance during the scan.

The specific capacitance of the electrode was calculated according to the equation [29]:

$$C = \frac{A}{v \times f \times m}$$

where C is the specific capacitance, A is the integral areas of the cyclic voltammogram loops, f is the scan rate, v is the voltage window, and m is the mass of the active material. The specific capacitance for these three types of supercapacitors all decreased with the scan rate increase (Fig. 4f). The loss of capacitance at high scan rates could be attributed to the delayed charge transfer following change of the electric field caused by the penetration and diffusion of electrolyte barrier into a relatively poor electronically or ionically conductive material [30-32]. The PTPT electrode delivered the lowest specific capacitance with 26 F g^{-1} at a scan rate of 5 mV s^{-1}. PPy and copolymer electrodes delivered a much higher specific capacitance, i.e., 216 and 291 F g^{-1} at a scan rate of 5 mV s^{-1}, respectively. The retained capacity was 6 F g^{-1} for PTPT at the scan rate of 500 mV s^{-1}, only about 23% of the initial capacitance, while 78% (166 F g^{-1}) and 70% (203 F g^{-1}) was retained for PPy and copolymer, respectively. These results clearly demonstrate that the copolymer delivered the highest specific capacitance at both the low and high scan rates.

Fig. 5a shows the Nyquist plots of supercapacitors based on PPy, PTPT and the copolymer taken in the frequency range from 100 kHz to 10 mHz at an equilibrium open circuit potential. In the high frequency domain (inset), a similar

semi-circle could be observed for PPy and the copolymer. The semicircle is associated with pseudo capacitance and the porous structure of the materials [33]. No obvious semi-circle was observed for PTPT, probably due to the limited Faradaic contribution from this film as evidenced by CV results [27]. In the low frequency region, the slope of PPy and copolymer supercapacitors tended to be a nearly vertical straight line, close to 90°, the characteristic of a pure capacitive behaviour. In the case of the PTPT system, the capacitive behaviour was replaced by the more inclined line which can be attributed to Warburg impedance that is associated with the diffusion limitation of ions in the active materials [34, 35].

The charge/discharge profiles of the symmetric supercapacitors composed of PTPT, PPy and the copolymer electrodes are presented in Fig. 6. The discharge capacitance per electrode can be calculated from the following equation [36]:

$$C_m = \frac{2Q}{\Delta V \times m} = \frac{2I \times t}{\Delta V \times m}$$

where C_m, I, t, ΔV and m are the discharge capacitance per electrode, the current of charge–discharge, time of discharge, charge/discharge potential windows and the amount of active material, respectively.

PTPT presented a small capacitance of 45 F g^{-1} at a current density of 0.5 A g^{-1} and decreased to 29 F g^{-1} at 4 A g^{-1}. Thus, this polymer was not investigated at higher discharge currents. The specific capacitance obtained at a current density of 0.5 A g^{-1} for copolymer and PPy were 279 and 227 F g^{-1}, respectively. Copolymer and PPy also demonstrated a good rate capability. The retained capacitance at current density of 10 A g^{-1} was still 254 and 219 F g^{-1} for copolymer and PPy, about 91% and 96% of that obtained at 0.5 A g^{-1}, respectively. This is further evidence of the efficient ion insertion/deinsertion in the active materials, and is consistent with the results from

cyclic voltammetry. As clearly shown in Fig. 7 the copolymer can deliver a higher energy density and power density than the PPy electrode in the applied current density range of 0.5-10 A g^{-1}. The maximum values of energy density and power density for copolymer were 36 Wh kg^{-1} and 6.5 kW kg^{-1}, while that for PPy was 24 Wh kg^{-1} and 6.4 kW kg^{-1}, respectively.

Discharge capacitance of these three types of electrodes as a function of the charge/discharge cycle number is shown in Fig. 8. PPy and copolymer were cycled at a current density of 5 A g^{-1}, while the PTPT was cycled at a current density of 1 A g^{-1}. PTPT showed a rapid drop of the capacitance, nearly 60% of its initial value was lost after 200 charge/discharge cycles. PPy exhibited a much better cycling stability, 84% of the initial capacitance remained after 1000 charge/discharge cycles. Copolymer delivered the best cycling stability, only a 9% capacitance decrease was observed under the same conditions.

All these results clearly demonstrated that the copolymer, as a supercapacitor electrode, possesses superior electrochemical properties including higher capacitance and better cycling stability. The addition of small amounts of PTPT (the mass ratio of PPy/TPT units was about 25:1 from element analysis) greatly improve the electrochemical properties of PPy, although PTPT itself is a very poor supercapacitor material. The introduction of PTPT into PPy may result in the production of a higher surface area, maximizing the electroactive surface and facilitating ion transport.

4.   Conclusion

In summary, the copolymer of pyrrole and 3-(4-*tert*butylphenyl)thiophene was synthesized via electropolymerization in acetonitrile with ClO_4^- as dopant. Though the homopolymer PTPT displayed very poor electrochemical properties, an introduction

of small amounts of TPT units leads to superior electrochemical properties in comparison with the homopolymer PPy or PTPT. It might be ascribed to the introduction of the PTPT units into PPy improved its available surface area. Copolymer delivered the highest capacitance of 291 and 203 F g^{-1} at a scan rate of 5 and 500 mV s^{-1}, in comparison with 216 and 166 F g^{-1} for PPy, 26 and 6 F g^{-1} for PTPT, respectively. In charge/discharge tests, the copolymer electrode exhibited a capacitance of 279 F g^{-1} at 0.5 A g^{-1}, much higher than that of PPy (227 F g^{-1}) and PTPT (45 F g^{-1}). The copolymer electrode also showed an improved cycling stability. After 1000 charge/discharge cycles at a current density of 5 A g^{-1} only a 9% decrease of capacitance was observed, while PTPT and PPy electrodes lost 60% and 16% of their initial capacitance, respectively.

References

[1] L. Nyholm, G. Nyström, A. Mihranyan, M. Strømme, Adv. Mater. 23 (2011) 3751-3769.

[2] B.E. Conway, Electrochemical Supercapacitors : Scientific Fundamentals and Technological Applications, Kluwer Academic/Plenum Publisher, New York, 1999.

[3] P. Novák, K. Müller, K.S.V. Santhanam, O. Haas, Chem. Rev. 97 (1997) 207-282.

[4] A. Rudge, I. Raistrick, S. Gottesfeld, J.P. Ferraris, Electrochim. Acta 39 (1994) 273-287.

[5] M.I.S. De Pinto, H.T. Mishima, B.A.L.P. De Mishima, J. Appl. Electrochem. 27 (1997) 831-838.

[6] H.E. Katz, P.C. Searson, T.O. Poehler, J. Mater. Res. 25 (2010) 1561-1574.

[7] G.A. Snook, P. Kao, A.S. Best, J. Power Sources 196 (2011) 1-12.

[8] B.C. Sih, M.O. Wolf, Chem. Commun. (2005) 3375-3384.

[9] R. Gangopadhyay, A. De, Chem. Mater. 12 (2000) 608-622.

[10] A. Malinauskas, J. Malinauskiene, A. Ramanavicius, Nanotechnology 16 (2005) R51-R62.

[11] R. Oliver, A. Munoz, C. Ocampo, C. Aleman, E. Armelin, F. Estrany, Chem. Phys. 328 (2006) 299-306.

[12] C. Zhang, C. Hua, G. Wang, M. Ouyang, C. Ma, Electrochim. Acta 55 (2010) 4103-4111.

[13] C. Zhang, Y. Xu, N. Wang, Y. Xu, W. Xiang, M. Ouyang, C. Ma, Electrochim. Acta 55 (2009) 13-18.

[14] J.Y. Liu, R. Zhang, G.V. Sauvé, T. Kowalewski, R.D. McCullough, J. Am. Chem. Soc. 130 (2008) 13167-13176.

[15] C.C. Chang, L.J. Her, J.L. Hong, Electrochim. Acta 50 (2005) 4461-4468.

[16] A.Q. Zhang, L.Z. Wang, L.S. Zhang, Y. Zhang, J. Appl. Polym. Sci. 115 (2010) 1881-1885.

[17] M.D. Stoller, R.S. Ruoff, Energy. Environ. Sci. 3 (2010) 1294-1301.

[18] R. Rajagopalan, J.O. Iroh, Electrochim. Acta 46 (2001) 2443-2455.

[19] R. Sasikumar, P. Manisankar, Polymer 52 (2011) 3710-3716.

[20] G.G. Wallace, G. Tsekouras, C. Wang, Inherently conducting polymers via electropolymerization for energy conversion and storage, in: S. Consnier, A. Karyakin (Eds.), Electropolymerization: Concepts, Materials and Applications, WILEY-VCH Verlag GmbH & Co. KGaA, Weinheim, 2010, pp. 215-240.

[21] N. Miyaura, A. Suzuki, Chem. Rev. 95 (1995) 2457-2483.

[22] D.J. Guerrero, X. Ren, J.P. Ferraris, Chem. Mater. 6 (1994) 1437-1443.

[23] C. Wang, W. Zheng, Z. Yue, C.O. Too, G.G. Wallace, Adv. Mater. 23 (2011) 3580-3584.

[24] Y.W. Chen-Yang, J.L. Li, T.L. Wu, W.S. Wang, T.F. Hon, Electrochim. Acta 49 (2004) 2031-2040.

[25] A. Gök, M. Omastová, A.G. Yavuz, Synth. Met. 157 (2007) 23-29.

[26] M. Omastová, M. Trchová, J. Kovářová, J. Stejskal, Synth. Met. 138 (2003) 447-455.

[27] Q. Wu, Y. Xu, Z. Yao, A. Liu, G. Shi, ACS Nano 4 (2010) 1963-1970.

[28] V. Khomenko, E. Raymundo-Pinero, E. Frackowiak, F. Beguin, Appl. Phys. A-Mater. 82 (2006) 567-573.

[29] X. Li, J. Rong, B. Wei, ACS Nano 4 (2010) 6039-6049.

[30] D. Pech, M. Brunet, H. Durou, P. Huang, V. Mochalin, Y. Gogotsi, P.-L. Taberna, P. Simon, Nat. Nanotechnol. 5 (2010) 651-654.

[31] C.C. Hu, K.H. Chang, M.C. Lin, Y.-T. Wu, Nano Lett. 6 (2006) 2690-2695.

[32] F. Meng, Y. Ding, Adv. Mater. 23 (2011) 4098-4102.

[33] J. Li, X. Wang, Y. Wang, Q. Huang, C. Dai, S. Gamboa, P.J. Sebastian, J. Non-Cryst. Solids 354 (2008) 19-24.

[34] S.B. Yoon, E.H. Yoon, K.B. Kim, J. Power Sources 196 (2011) 10791-10797.

[35] Q. Wang, Z. Wen, J. Li, Adv. Funct. Mater. 16 (2006) 2141-2146.

[36] Q.F. Wu, K.X. He, H.Y. Mi, X.G. Zhang, Mater. Chem. Phys. 101 (2007) 367-371.

Captions

Fig. 1 Chronopotentiograms for the deposition of PTPT (i), Copolymer (ii) and PPy (iii) at a current density of 0.5 mA cm^{-2}, on stainless steel mesh from an acetonitrile solution containing 0.02 M monomer and 0.1 M LiClO$_4$.

Fig. 2 SEM images of PPy (a, d), copolymer (b, e) and PTPT (c, f) films.

Fig. 3 FTIR spectra of PTPT (i), copolymer (ii) and PPy films (iii).

Fig. 4 Cyclic voltammograms of PTPT (a), PPy (b) and copolymer (c) symmetric supercapacitors at different scan rates. (d) Cyclic voltammograms of symmetric capacitors based on PTPT (i), PPy (ii) and copolymer (iii) at a scan rate of 100 mV s^{-1}. (e) Specific capacitance obtained at different scan rates for PTPT, PPy and copolymer based supercapacitors (calculated from CV).

Fig. 5 Nyquist plots of symmetric supercapacitors based on PTPT (i), PPy (ii) and copolymer (iii) films. Inset, expanded view of the Nyquist plots at high frequency.

Fig. 6 Charge/discharge curves of PTPT (a), PPy (b) and copolymer (c) based supercapacitors at different current densities: 0.5 (i), 1 (ii), 2 (iii) and 5 A g^{-1} (4 A g^{-1} for PTPT supercapacitor) (iv). (d) Discharge capacitance versus current density for PTPT (i), PPy (ii) and copolymer (iii) based supercapacitors.

Fig. 7 Ragone plots for PPy and copolymer based supercapacitors.

Fig. 8 Discharge capacitance versus cycle number for PPy and copolymer based supercapacitors at a current density of 5 A g^{-1}, while a current density of 1 A g^{-1} was applied for PTPT based supercapacitors.
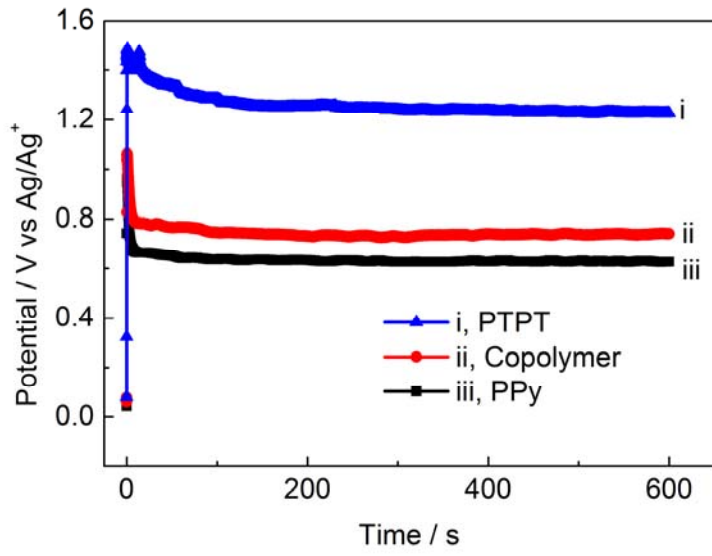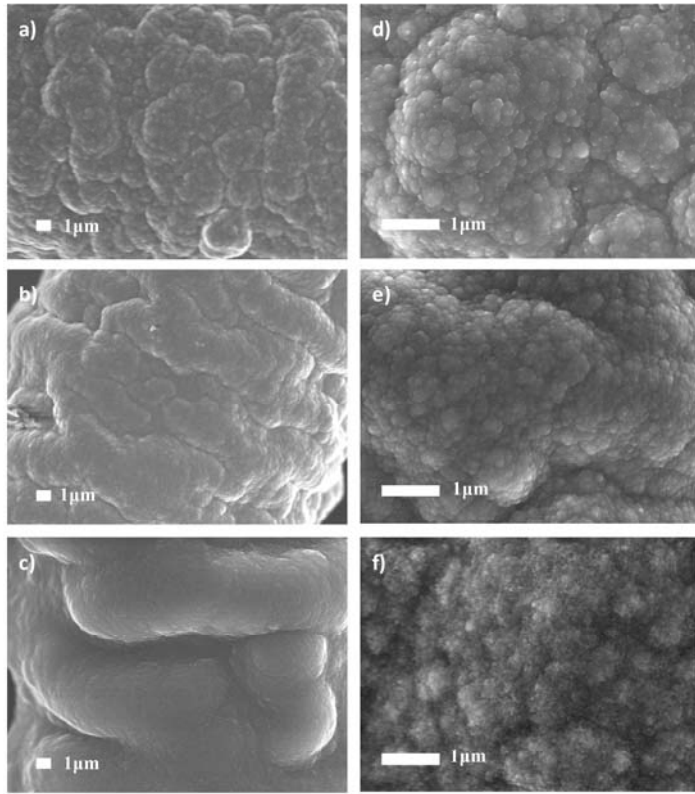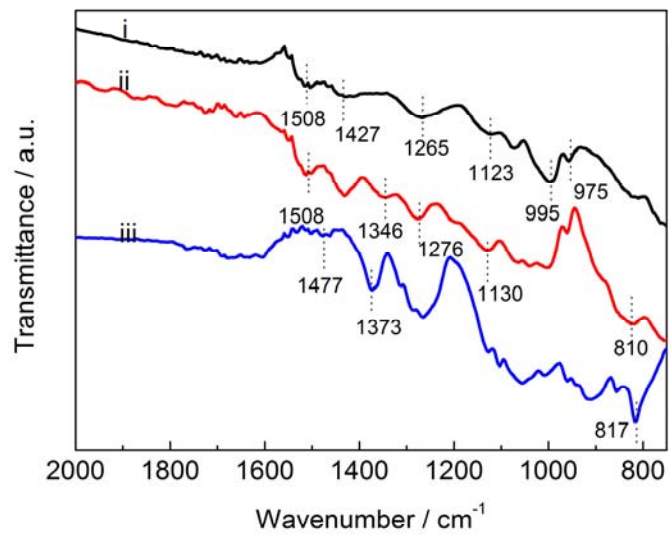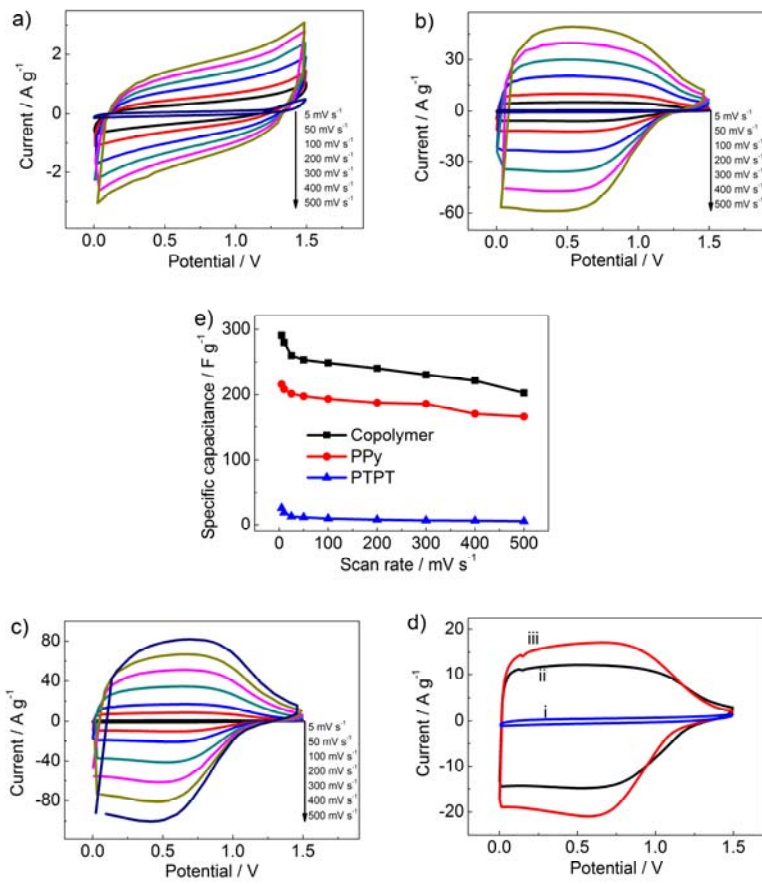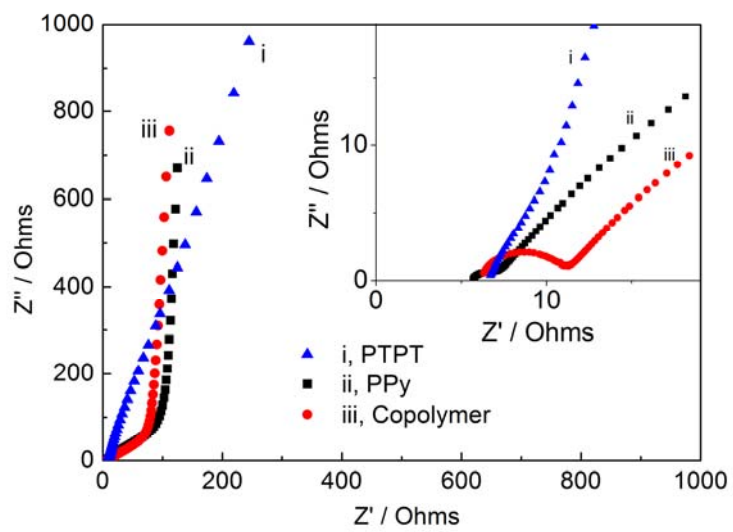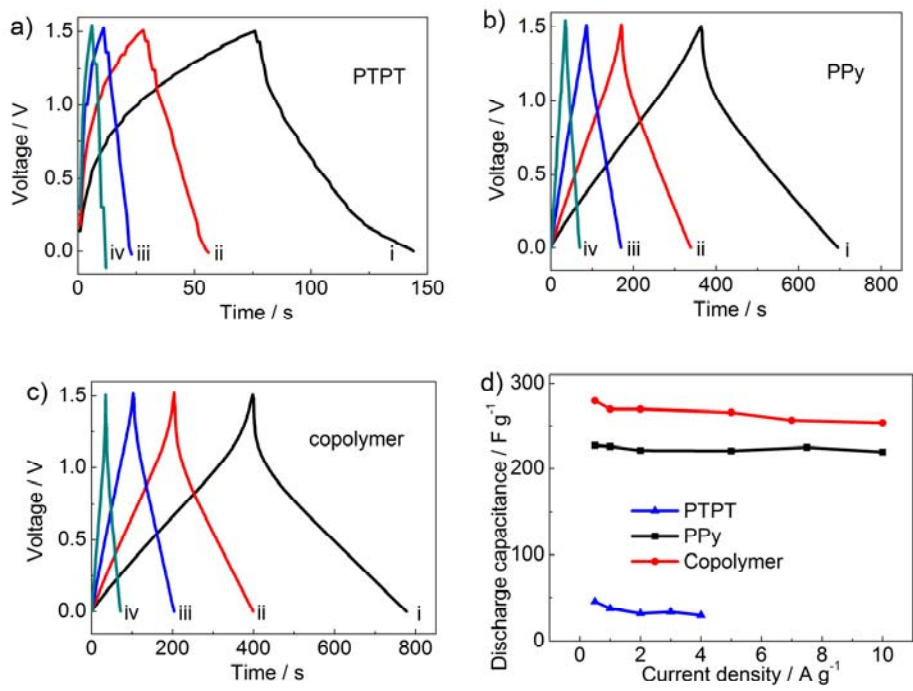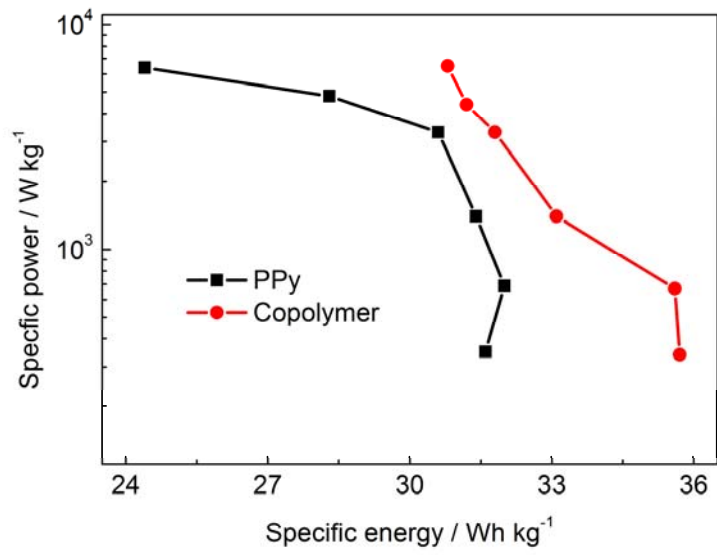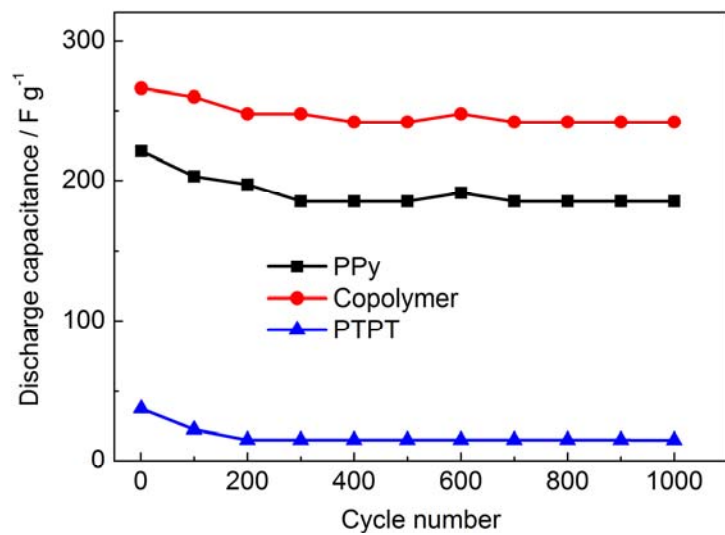
Figure 1

Figure 2

Figure 3

Figure 4

Figure 5

Figure 6

Figure 7

Figure 8